Simulation-based Thermohydrodynamic Analysis of a Claus Process Catalytic Reactor

R. Muthalathu[1] T. Treeratanaphitak[2] E. Nasato[3]
N.M. Abukhdeir[1,4]

[1]Dept. of Chemical Engineering, University of Waterloo, Waterloo, Ontario, Canada
[2]Sirindhorn International Institute of Technology, Thammasat University, Pathum Thani, Thailand
[3]Nasato Consulting Ltd., Oakville, Ontario, Canada [4]Continuum Engineering Inc., Waterloo, Ontario, Canada September 7, 2025

1 Introduction

Catalytic reactor units (CRUs) are a key component of sulfur recovery units (SRUs) based on the Claus process (Figure 1) and, where applicable, hydrogenation tail gas reactions. CRUs involve process gas being fed through an insulated packed bed reactor with a supported catalyst which promotes the exothermic Claus process-related reactions,

$$2\,H_2S + SO_2 \rightleftharpoons S_n + 2\,H_2O \text{ where } n = 2, 6, 8$$

Reheating involves significant operating costs, but catalytic reaction and condensers pose operational challenges.

Typical hydrodynamic conditions in industrial scale catalytic reactors (Figure 2a) result in turbulent flow both within inlet/outlet void spaces and within a multilayer supported catalyst bed. The catalyst bed inlet temperature is a process set-point such that, under normal operating conditions, a desired reaction conversion is achieved. However, depending on the design and operating conditions (normal, turn-down, co-firing, etc) significant heat losses and temperature variations within the catalytic bed may occur. Additionally, hydrodynamic conditions resulting from particular reactor designs (Figure 2b) are known to increase risk for catalyst displacement. These variations might result in reduced sulfur recovery efficiency, requiring increased heat duty of reheaters, or even result in operational and reliability risks due to potentially corrosive cold zones.

The typical Claus process catalytic reactor, where a two-bed reactor is shown in Figure 2a, has three different regions:

1. *single-phase inlet* region where, ideally, there is simple unidirectional diverging flow from single or multiple inlets with gas distribution features (Figure 2c) to the catalyst bed.

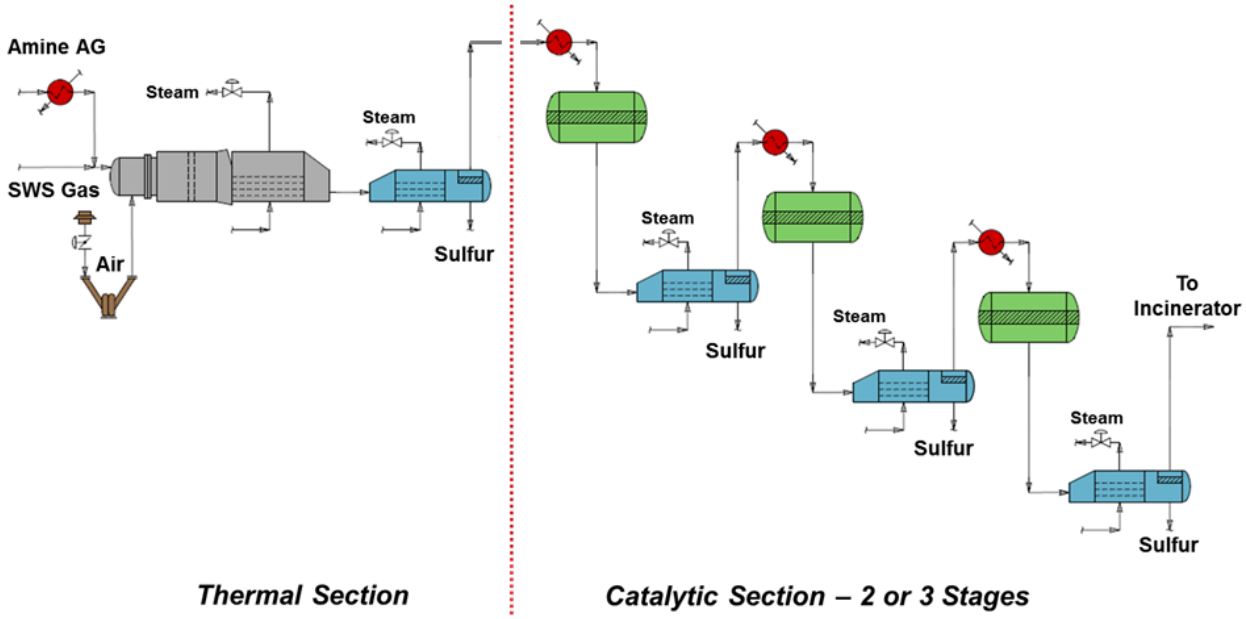

Figure 1: Schematic flow diagram of a typical straight-through Claus Sulfur Recovery Unit (SRU) with catalytic recovery consisting of reheating, catalytic reaction, and condensation/separation. Taken from reference [1].

2. *multiphase catalyst bed* region in which there are multiple upper and lower layers of inert particles to protect and support a central (interior) layer of catalyst particles.

3. *single-phase outlet* region where, ideally, there is simple converging flow from the catalyst bed to a single or multiple outlets.

The number and geometry of reactor inlets along with the catalyst bed layer thickness and particle sizes are key design decisions which affect the cost, catalytic performance, pressure drop, and reliability of catalytic reactors. Current trends in the operation of SRUs motivate increasingly long intervals between shutdowns, which necessitate increasingly reliable reactor designs. Poor designs and/or deviation from expected operating conditions can result in catalyst displacement both within and without the catalyst bed, with a real-world example shown in Figure 2d, which increases operational and reliability risks.

In this work, simulation-based analysis using a coupled multiphase hydrodynamic and thermal model, referred to as a *multiphysics* model, is performed for a representative industrial-scale Claus catalytic reactor. Past applied research studies and limited experimental process measurements have been provided in the literature for this industrial-scale unit [2], used for limited validation of simulations. A standard method for feed gas distribution is evaluated, the use of multiple inlets in combination with inlet deflection plates, to understand the benefits and drawbacks of feed gas distribution under normal operating conditions. Simulations are fully three-dimensional and transient, performed using a combination of compressible turbulent flow and inertia-dominated flow in porous media (Darcy-Forchheimer) models. Porous media transport properties were estimated using the provided typical catalyst loading schemes used in most SRUs combined with empirically determined correlations

of Forchheimer coefficients for uniform diameter (simple, monodisperse) randomly-packed spheres.

Analysis of simulation-predicted gas flow distribution, temperature variation, and heat loss were performed for both single-phase inlet/outlet regions and the porous catalyst bed space under normal operating conditions. Simulations predict gas flow throughout the catalyst bed to be nearly ideal uniform and unidirectional. However, depending on inlet flow distribution conditions, flow within the inlet region is non-uniform and involves significant recirculation and stagnation in multiple regions. This is found to result in the potential for relatively high shear stresses at the upper surface of the catalyst bed and non-uniform temperature/heat transfer within catalyst bed. Non-uniform inlet distribution of the feed gas is also found to significantly increase the potential for catalyst displacement, effect heat transfer and temperature distribution within the catalytic reactor, varying depending on operating condition and the corresponding different in feed flowrate, temperature, and composition.

Additionally, thermal-reaction analysis was performed for selected Claus reactor designs under normal operating conditions. Simulation results were found to agree well with industrial process measurements, validating the model and simulation methods used. Intraphase heat transfer within the catalyst bed was found to be highly coupled with pre-heating and exothermic reaction regions undergoing inter- and intraphase heat exchange. Furthermore, the improved inlet distribution of the process gas resulting from the use of inlet impingement plates was shown to result in a modest increase in reaction conversion.

2 Theory and Numerical Methods

The three different regions of a Claus reactor (inlet, catalyst bed, outlet) involve single-phase compressible turbulent flow (inlet and outlet) and multiphase flow through porous media (catalyst bed). The modelling method used in this work involves decomposing the reactor into these three regions and using the most appropriate model, with respect to accuracy and computational efficiency, within each sub-domain. Consequently, standard interior boundary conditions are introduced coupling transport and mass, momentum, and energy which are not included for brevity. Additionally, radiative heat transfer is neglected and not expected to significantly affect results based on a scaling analysis using the Stefan-Boltzmann law and the two characteristic temperatures associated with normal operating conditions (inlet and catalyst bed temperature).

2.1 Multiphase Hydrodynamics

Single-phase compressible turbulent flow in the inlet and outlet regions was modelled using the compressible Favre-averaged Navier-Stokes (FANS) equations, which use density weighted time averaging ($\widetilde{\phi}$) versus classical time-averaging ($\bar{\phi}$) used for incompressible turbulent flows (Reynolds-averaged Navier-Stokes equations). For brevity only the mixture equations are shown, with component mass conservation equations, reaction terms, and tur-

bulence models excluded [3]:

$$\frac{\partial \bar{\rho}}{\partial t} + \nabla \cdot (\bar{\rho}\widetilde{\boldsymbol{u}}) = 0 \tag{1}$$

$$\frac{\partial \bar{\rho}\widetilde{\boldsymbol{u}}}{\partial t} + \nabla \cdot \left[\bar{\rho}\widetilde{\boldsymbol{u}}\widetilde{\boldsymbol{u}} + \bar{p}\boldsymbol{\delta} - \widetilde{\boldsymbol{\tau}^{lam}} - \widetilde{\boldsymbol{\tau}^{turb}}\right] = 0 \tag{2}$$

which assume a perfect gas (ideal gas with constant heat capacity). The conservation of energy, excluding reaction terms is as follows,

$$\frac{\partial \bar{\rho}\widetilde{e_0}}{\partial t} + \nabla \cdot \left[\bar{\rho}\widetilde{\boldsymbol{u}}\widetilde{e_0} + \widetilde{\boldsymbol{u}}\bar{p} + \widetilde{\boldsymbol{q}^{lam}} + \widetilde{\boldsymbol{q}^{turb}} - \widetilde{\boldsymbol{u}} \cdot \left(\widetilde{\boldsymbol{\tau}^{lam}} - \widetilde{\boldsymbol{\tau}^{turb}}\right)\right] \tag{3}$$

with the density-averaged total energy given by,

$$\widetilde{e_0} = \tilde{e} + \frac{1}{2}\widetilde{\boldsymbol{u}}\widetilde{\boldsymbol{u}} + k \tag{4}$$

where k is the turbulent kinetic energy. Additional approximations and sub-models used include:

- ideal gas law equation of state,
- JANAF empirical relations [4] for thermodynamic properties (heat capacity),
- Sutherland law [5] for dynamic viscosity,
- mass-fraction weighted mixing to the thermodynamic coefficients,
- Wilke equation-based mixing [6] for transport properties,
- $k - \epsilon$ turbulence model [7]

Fluid flow through porous media was modelled using the Darcy-Forchheimer model with the Ergun equation [8] used to relate pressure gradient and fluid velocity,

$$\frac{\partial \rho \boldsymbol{u}}{\partial t} + \nabla \cdot (\rho \boldsymbol{u}\boldsymbol{u}) = \frac{A\alpha\mu}{d^2}v + \frac{B\beta\rho}{d}\boldsymbol{u} \cdot \boldsymbol{u} \tag{5}$$

$$\alpha = \frac{(1-\epsilon)^2}{\epsilon^3} \text{ and } \beta = \frac{(1-\epsilon)}{\epsilon^3} \tag{6}$$

where A/B are dimensionless constants, μ/ρ is the dynamic viscosity/density of the fluid phase, d is mean particle diameter, and ϵ is the porosity of the porous medium. The dimensionless constants A and B varying depending on the fluid flow regime within the porous medium, shown in Figure 3. For Claus reactors fluid flow within the porous catalyst bed is well-within the turbulent flow regime $Re \gg 2000$. This simplifies flow parameters in that they become constant with respect to fluid velocity based on past experimental research [9].

An open-source implementation of the FANS and Darcy-Forchheimer models with supporting closures is used as provided by the OpenFOAM simulation software package (version 11) [10], which enables external verification of the presented results through the use of an open-access simulation software.

3 Results and Discussion

This simulation study is based on a Claus SRU design and operating conditions from past work of Zughbi and Razzak [2], which provides both real-world operating data and multi-physics simulations of a multi-inlet Claus SRU with dimensions shown in Figure 4. Normal operating conditions, based on real-world data, involved an inlet mass flowrate of approximately $50kg/s$ which corresponds to an inlet superficial velocity of $57m/s$ for a three-inlet case. Experimentally measured inlet and outlet temperatures and component mass fractions (H_2S, SO_2, and H_2O) are shown in Table 1.

Table 1: Industrially measurements and past simulation predictions for inlet/outlet process gas conditions, take from ref. [2]

	Inlet industrial	*Outlet* industrial	*Outlet* simulation
Temperature (K)	511	572	575
H_2S Mass Frac.	0.0638	0.0159	0.0153
SO_2 Mass Frac.	0.0608	0.0149	0.0152
H_2O Mass Frac.	0.0440	0.0748	0.0716
S_2 Mass Frac.	0		0.0113
S_6 Mass Frac.	0		0.0213
S_8 Mass Frac.	0		0.0401

Past work indicated that the catalyst bed was composed of $1.4m$ of 1/8" diameter spherical catalyst particles, however, this would not be mechanically stable and it is assumed that inert support layers were neglected to reduce computational complexity. In this work, simulations are performed assuming a catalyst bed configuration representative of real-world conditions with top/bottom inert support layers and an inert flow distribution layer above the catalyst layer (as-specified in previous work). From top to bottom, the catalyst bed configuration used in all simulations is:

- *upper support layer* $0.15m$ of 3/8" inert support
- *flow distribution layer* $0.4m$ of 3/16" inert distribution
- *catalyst layer* $1.4m$ of 1/8" catalyst
- *lower support layer* $0.15m$ of 1/2" inert support

The catalytic reactions can be modelled using non-elementary power-law rate expressions with the reaction rate constants approximated using the Arrhenius equation,

$$R_i = Ae^{-E/RT}T^{\beta}f([i]) \tag{7}$$

where R_i is the rate of reaction, A is the Arrhenius constant, R is the gas constant, E is activation energy, T is temperature, β is a dimensionless exponent, and $f([i])$ is the rate law

expression [2]. The reaction rate expressions used in ref. [2] were based computationally-motivated simplifications of empirically-determined rates expressions [11] for the three reversible reactions representing the formation of different sulphur allotropes (S_2, S_6 and S_8),

$$R_{H2S} = \exp\left(\frac{-30594}{8.3145T}\right) T^{-0.7} C_{\mathrm{H_2\ S}} C_{\mathrm{SO_2}}^{0.7} C_{\mathrm{H_2O}}{}^{-2} C_{\mathrm{S_2}}{}^{0} \tag{8}$$

$$R_{H2S} = \exp\left(\frac{-30594}{8.3145T}\right) T^{-0.5} C_{\mathrm{H_2\ S}} C_{\mathrm{SO_2}}^{0.7} C_{\mathrm{H_2O}}{}^{-2} C_{\mathrm{S_6}}{}^{0} \tag{9}$$

$$R_{H2S} = \exp\left(\frac{-30594}{8.3145T}\right) T^{-0.4} C_{\mathrm{H_2\ S}} C_{\mathrm{SO_2}}^{0.7} C_{\mathrm{H_2O}}{}^{-2} C_{\mathrm{S_8}}{}^{0} \tag{10}$$

in units ($kmol/sm^3$). It is noted that S_2 formation is expected only at higher temperatures present in Claus CRUs, but the reaction is included in past and current simulations for completeness.

The presented simulation study involves two separate sub-studies under normal operating conditions:

1. A *hydrodynamic* analysis of inlet flow distribution through the use of multiple inlets (1, 2 and 3) and inlet impingement plates.

2. A *thermal-reaction* analysis of spatial variation in catalyst bed temperature and reaction rate, along with overall reaction conversion.

3.1 Hydrodynamic Analysis

In order to study the effect of inlet flow distribution into the catalytic bed of the Claus reactor, simulations were performed under normal operating conditions. Reactor configurations with single, dual, and triple inlets with inlet flow equally distributed between them were evaluated. Initial simulations were performed using a commensurate inlets configuration as in ref. [2], without an inlet impingement plate. Simulations were performed without chemical reactions enabled, in order to reduce computational cost given the focus on hydrodynamics in this part of the study. Simulations visualization of developed flows within the reactor designs are shown in Figures 5 and 6 which use velocity streamlines and the line integral convolution (LIC) method [12], respectively.

Focusing on the single-inlet reactor design, shown in Figures 5a and 6a, the absence of a standard inlet impingement plate results in the catalyst bed surface below the inlet acting to deflect and redirect the inlet flow. Conceptually, the ideal flow profile in the inlet region would be one that smoothly diverges from the inlet equally to all areas of the surface of the catalyst bed. Instead, the single-inlet design results in a significant amount of recirculation directly below the inlet with axial flows to both ends of the inlet region that are redirected into the catalyst bed. The use of the catalyst bed to redirect inlet flow is undesirable due to the potential for displacement of inert supports particles and resulting mechanical instabilities resulting from "short-circuiting" of process gas through sub-regions of the bed.

However, assuming no displacement of the catalyst bed, the flow profile through it is found to mitigate the complex inlet region flow imposed by the single-inlet, with quasi-ideal distribution of the inlet flow observed within the bed. The outlet region is predicted to have

an almost ideal converging flow from the catalyst bed to the single outlet, which is intuitive given the almost ideal distribution of flow entering the outlet region.

Focusing on the dual and triple-inlet reactor designs, shown in Figures 5b-c and 6b-c, similar flow profiles are observed below the inlets due to the absence of a standard inlet impingement plate. The catalyst bed surface below each inlet acts to deflect and redirect the inlet flow. However, there is a reduction in axial flow from each inlet recirculatory region as the number of inlets increases and flow is distributed spatially along the catalyst bed, as compared to the single-inlet case. Comparing the velocity LIC visualizations for the dual and triple inlet designs, shown in Figures 6b-c, a significant reduction in the amount of recirculation below the inlets is observed where recirculation is almost absent for the triple-inlet case. Additionally, increasing the number of inlets is observed to segregate inlet flow, such that it is expected that the residence time distribution (RTD) will be closer to ideal and less diffuse. However, RTD simulations were not performed in this study or past studies. Flow behavior in the catalyst bed and outlet regions for the dual and triple inlet designs was found to be almost identical to the single inlet design.

Based on the desirable inlet flow distribution performance of the triple inlet design, the effect of inlet impingement plates was studied through performing simulations for the triple inlet with their addition. Figure 7 shows velocity streamline and LIC visualizations for the triple inlet case with impingement plates. The velocity profile is more complex than that of the original design, with the inlet flow being equally divided between each of the three inlets, then further divided axially by each of the three impingement plates. This results in redirection from axial to downwards flow both at the ends of the reactor and in between pairs of inlets. This results in the presence of an equal number of recirculatory regions compared to the design without impingement plates (6 total). Thus, based on velocity profiles alone, a distinction between the two designs is not apparent and requires further analysis.

Current and past simulations assume the catalyst bed is not deformable and that inert and catalyst particles are not put in motion in response to stresses imposed by process gas flow. In order to understand the validity of that assumption and, simultaneously, leverage simulation results to predict whether or not each design could result in potential catalyst bed displacement, a simple scaling analysis was performed. Inert particles composing the first layer of the catalyst bed are exposed to three different forces: (i) gravitational force, (ii) hydrodynamic force (process gas), and (iii) static forces from catalyst particles below. In order for an inert particle to be displaced, focusing on entrainment into the process gas flow of the inlet region, gravitational force on the particle,

$$\boldsymbol{f}_g = \rho_s V_s g_c \boldsymbol{z} \tag{11}$$

must be overcome by hydrodynamic force from the process gas,

$$\boldsymbol{f}_h = \boldsymbol{z} \cdot \left(\int_A \boldsymbol{n} \cdot \boldsymbol{\tau} dA \right) \boldsymbol{z} \tag{12}$$

where ρ_s is the density of the particle, V_s/A is its volume/area, g_c acceleration due to gravity, $\boldsymbol{z}$ is the direction of gravity (vertical), $\boldsymbol{n}$ is the unit normal to the surface of the catalyst, and τ is the viscous stress tensor. However, further approximation is required to estimate $\boldsymbol{f}_h$

given that the modelling approach used in this and past work predicts the volume-averaged stress in the vicinity of catalyst particles and thus,

$$\boldsymbol{f}_h \approx A_s \left(\boldsymbol{z} \cdot \bar{\boldsymbol{\tau}}\right) = A_s \left(\boldsymbol{t}_{normal} + \boldsymbol{t}_{shear}\right) = \boldsymbol{f}_{normal} + \boldsymbol{f}_{shear} \tag{13}$$

where A_s is the surface area of the particle, $\boldsymbol{t}_{normal}/\boldsymbol{t}_{shear}$ are the normal and shear components of the surface traction, and $\boldsymbol{f}_{normal}/\boldsymbol{f}_{shear}$ are the corresponding components of the hydrodynamic force on the particle.

A comparison of the gravitational and hydrodynamic forces, based on the simulation-predicted viscous stress at the catalyst bed surface, was performed for the 3/8" catalyst particles assuming a density of $4000kg/m^3$. The direction of hydrodynamic forces was accounted for, such that forces were compared in the upwards and downwards directions, where the latter corresponds to that of gravitational force. Table 2 shows results for each of the reactor designs along with the ratio of upwards to downwards forces, which leads to the following observations:

1. For all designs, hydrodynamic forces are not predicted to be sufficient to entrain inert support particles into the process gas flow of the inlet region.

2. Improving the distribution of inlet flow through increasing the number of inlets significantly reduces upwards forces on particles.

3. The addition of inlet baffles, for the same number of inlets, further reduces forces on particles on the upper surface of the catalyst bed.

Figures 8-9 show simulation predictions of the hydrodynamic stress at the catalyst bed surface for both triple-inlet simulations, without and with inlet baffles. Addition of the inlet baffles results in a near ideal distribution of significantly reduced stresses over the catalyst bed surface. There is also an absence of inversion of normal stress from downwards to upwards with overall increase in downwards force on the support particles.

Table 2: Comparison of upwards and downwards forces on the top layer of inert catalyst particles as predicted by simulations.

	1 Inlet	2 Inlet	3 Inlet	3 Inlet Baffled
$\boldsymbol{f}_{down}$	$0.0177N$	$0.0177N$	$0.2777N$	$0.4377N$
$\boldsymbol{f}_{up}$	$0.000899N$	$0.0003509N$	$0.0001653N$	$0.0000377N$
$\boldsymbol{f}_{up}/\boldsymbol{f}_{down}$	0.05	0.02	0.0006	0.0003

3.2 Thermal-Reaction Analysis

In order to study the thermal-reaction performance of the Claus reactor design, simulations were performed under normal operating conditions for reactor configurations only with triple inlets, with and without inlet impingement plates, with inlet flow equally distributed between them. Triple-inlet Claus reactor configurations were focused on due to their improved inlet distribution and reduced catalyst bed surface stresses, as determined in the

previous section. Simulations were performed with both chemical reactions and interphase heat transfer, between the porous catalyst bed and process gas, resulting in relatively computationally intensive three-dimensional transient simulations. Simulations were performed until steady-state was achieved, based on outlet mass/energy flowrates and internal composition/temperature profiles. Spatial variation in catalyst bed temperature and mass fraction, along with overall reaction conversion, was then analyzed. Difference in pressure drop was also estimated based on steady-state results, with the addition of inlet baffles predicted to increase pressure drop by approximation 350Pa (0.05psi).

Simulations visualizations of catalyst bed temperature and exit H_2S composition are shown in Figures 10-11. Spatial variation of temperature within the solid porous catalyst bed phase is predicted to vary only slightly in the vertical direction, as seen in Figures 10a,b. For both designs, temperature within the solid porous phase of the catalyst bed varies only slightly from outlet conditions and localized in the upper region. Comparing temperature profiles for the designs without and with inlet impingement plates, there is significantly more variation of temperature within the plane of the surface of the bed for the design without impingement plates. Focusing on Figure 10a, horizontal variation mirroring the location of the process gas inlets is observed, which is not the case for the design with impingement plates (10b) However, the only significant temperature variation of the for both the porous solid and gas phases is within the initial 0.15m of the bed, where the largest diameter (3/8") inert support is located. Figures 10c,d show horizontal cross-sections of the process gas temperature within the inert distribution layer, where rapid heat transfer from the solid-to-gas phase occurs which is referred to as "pre-heating." Overall, the lack of inlet impingement plates results in slightly lower rate of pre-heating in the design without impingement plates, but overall the desirable distribution properties of the inert upper layers (support and distribution layers) mitigates the poorer inlet process distribution of this design issue.

Simulation-based observations of the temperature profiles within the porous catalyst phase and the process gas phase provide significant insight into the heat transfer within the reactor. The upper support and distribution layers of inert particles not only serve to distribute inlet flow but also preheat it prior to entering the catalyst layer through heat transfer from porous solid to gas phase. Exothermic reaction in the process gas within the catalyst layer results in an inversion of heat transfer from gas to porous solid phase. Conductive heat transfer within the solid porous phase is couples these two regions through heat transfer from the high temperature reaction zone to the lower temperature inlet zone.

Spatial variation of H_2S mass fraction at the outlet of the catalyst bed is shown for both designs in Figures 11a,b. Outlet composition around the perimeter of the bed is lowest, due to the relatively lower velocities in this region resulting from no-slip conditions at the reactor shell. Spatial variation of H_2S composition is relatively similar for both design cases, due to the high rate of of conversion and quasi-ideal distribution characteristics of the porous solid catalyst bed. The use if impingement plates is not found to result in significantly different outlet compositions of the process gas, apart from the more rapid pre-heating described previously.

In order to determine overall reaction conversion predicted by simulations of the triple inlet designs and quantitatively compare with process data, outlet compositions ω_{H_2S} and

ω_{S_X} were determined based on mass flowrates at the outlet,

$$\omega_i = \frac{\int_{A_o} \rho\omega_i \left(\boldsymbol{n}\cdot\boldsymbol{v}\right) dA_o}{\int_{A_o} \rho \left(\boldsymbol{n}\cdot\boldsymbol{v}\right) dA_o} \tag{14}$$

where $\boldsymbol{v}$ is the fluid velocity and $\boldsymbol{n}$ is the unit normal (outwards) of the surface. Reaction conversion is formulated based on H_2S being the limiting component,

$$\eta_{H_2S} = 1 - \frac{\int_{A_o} \rho\omega_{H_2S} \left(\boldsymbol{n}\cdot\boldsymbol{v}\right) dA_o}{\int_{A_i} \rho\omega_{H_2S} \left(\boldsymbol{n}\cdot\boldsymbol{v}\right) dA_i}. \tag{15}$$

In order to compare to past industrial and simulation-based reaction conversion data from ref. [2] outlet compositions were *assumed* to be mass-averaged. Thus, taking into account steady-state operation,

$$\eta_{H_2S} = 1 - \frac{\omega_{H_2S,o}}{\omega_{H_2S,i}}. \tag{16}$$

Table 3 shows a comparison of industrial and simulation results for reactor outlet temperature, reaction conversion, and composition. Simulation results from ref. [2] are shown for illustrative purposes and not compared in this discussion due to prediction of anomalous reaction conversion of S_2 which is not expected to be producted in high compositions outside of the thermal section of the SRU. Comparing industrial data to simulation predictions without and with inlet impingement plates, both simulation results show reasonable agreement lending to some degree of validation of the model and simulation method. Both simulations shown slightly lower outlet process gas temperatures compared to industrial data, with higher reaction conversions. As expected, rate of production of S_6 and S_8 far exceed that of S_2, as is expected by past research and industrial observations in the catalytic section [1]. Comparing simulations of the original design of the CRU being studied to the modified design with inlet impingement plates, it is seen that the improved distribution of process gas at the inlet yields a slight improvement in reaction conversation. This can be attributed to a slightly more rapid pre-heating effect at the inlet of the catalyst bed, shown in Figure 10.

Table 3: Comparison of outlet process gas conditions from industrially measurements [2], past simulations [2], and present simulations.

	industrial	simulation ref. [2]	simulation 3 inlet	simulation 3 inlet (imp.)
Temperature (K)	572	575	570.7	571.3
Conversion (η_{H_2S})	0.751	0.761	0.815	0.815
H_2S Mass Frac.	0.0159	0.0153	0.0120	0.0118
SO_2 Mass Frac.	0.0149	0.0152	0.0120	0.0118
H_2O Mass Frac.	0.0748	0.0716	0.0716	0.0715
S_2 Mass Frac.		0.0113	0.0001	0.0001
S_6 Mass Frac.		0.0213	0.0253	0.0254
S_8 Mass Frac.		0.0401	0.0477	0.0479

4 Conclusions

A simulation-based analysis of an industrial-scale Claus catalytic reactor unit (CRU) was performed a using three-dimensional transient multiphase multiphysics simulations. Past applied research studies and industrial process measurements [2] were used both as a basis for simulations and for some degree of experimental validation of results. The study was composed of two sequential sub-studies: (i) a hydrodynamic analysis of inlet flow distribution through the use of multiple inlets and inlet impingement plates, (ii) a thermal-reaction analysis of spatial variation in catalyst bed temperature, reaction rate, and overall reaction conversion.

The use of increasing numbers of equally distributed inlets for process gas distribution was found to both reduce recirculation and hydrodynamic stresses in the inlet region of the CRU. The catalyst bed was found to effectively distribute process gas, regardless of inlet region distribution. However, poor distribution of inlet process gas was found to impart significant hydrodynamic stresses on the catalyst bed surface and be detrimental to uniform heat transfer in the upper region of the catalyst bed. The use of inlet impingement plates was also studied, finding that their addition significantly reduces surface stresses on the catalyst bed, but does not remove the presence of recirculation zones within the inlet region. These results motivate further study of process gas distribution features which involve increasing number of inlets in order to both improve distribution of hydrodynamic stress on the catalyst surface and further reduce recirculatory zones in the inlet region of the CRU. Further improvements in process gas distribution could have the desirable effects of reducing the potential for mechanically disturbing the catalyst bed while simultaneously improving mass/heat transfer uniformity. This will be especially important for abnormal operations such as turndown, co-firing and hot-standby. In addition, this level of modeling will assist with modification of reactor inlet deflector designs that are prone to catalyst displacement.

Thermal-reaction analysis was performed for the three-inlet Claus reactor designs, due to there improved performance in distribution of inlet process gas. Simulations were performed under normal operating conditions for reactor configurations and were found to agree well with industrial process measurements, validating the model and simulation methods used. Intraphase heat transfer within the catalyst bed and interphase heat transfer between it and the process gas was found to be highly coupled. The porous solid catalyst bed phase was found to be relatively uniform in temperature close to that of the outlet process gas. Within the inert upper support and flow distribution layers of the catalyst bed, the process gas was observed to be pre-heated prior to entering the catalyst layer. Within the catalyst layer, the exothermic reaction within the gas phase was found to result in heating of the solid catalyst, with conductive heat transfer within the solid phase effectively closing a heat transfer "loop" within the catalyst bed region of the CRU. Additionally, the improved inlet distribution of the process gas resulting from the use of inlet impingement plates was shown to result in a slight increase in reaction conversion.

Simulation-based analysis of catalytic reactors present in Claus processes is a promising predictive tool for assessment of the performance of existing units and their design. Innovations in catalytic reactor design, including inlet flow distribution, have the potential to result in increased extended catalytic reactor performance and reliability under all relevant operating conditions, while simultaneously reducing operating costs associated with high

reheater duty and/or premature SRU shutdown due to poor catalytic performance.

References

[1] None. Proceedings of the lawrence reid gas conditioning conference. None, University of Oklahoma Press,Norman, OK, 12 1985. URL https://www.osti.gov/biblio/6758229.

[2] Habib Daoud Zughbi and Shaikh Abdur Razzak. Simulation of flow and chemical reactions in a claus sulfur converter. *Industrial & engineering chemistry research*, 44 (26):9828–9839, 2005.

[3] Epaminondas Mastorakos and R Stewart Cant. *An introduction to turbulent reacting flows*. World Scientific Publishing Company, 2007.

[4] Jr. M.W. Chase, C.A. Davies, Jr J.R. Downey, D.J. Frurip, R.A. McDonald, and A.N. SyverudLen Thomas. Nist-janaf thermochemical tables, 1998. https://janaf.nist.gov/.

[5] William Sutherland. Xxxvii. the viscosity of mixed gases. *The London, Edinburgh, and Dublin Philosophical Magazine and Journal of Science*, 40(246):421–431, 1895.

[6] Henry Cheung, Leroy A Bromley, and CR Wilke. Thermal conductivity of gas mixtures. *AIChE Journal*, 8(2):221–228, 1962.

[7] David Ting. *Basics of engineering turbulence*. Academic Press, 2016.

[8] Maasoud Kaviany. *Principles of heat transfer in porous media*. Springer Science & Business Media, 2012.

[9] RM Fand, BYK Kim, ACC Lam, and RT Phan. Resistance to the flow of fluids through simple and complex porous media whose matrices are composed of randomly packed spheres. *Journal of fluids engineering*, 109(3):268–273, 1987.

[10] OpenFOAM Foundation. Openfoam v11, 2023. https://openfoam.org/release/11/.

[11] DA Abaskuliev, NM Guseinov, and A Ch Mekhraliev. Mathematical model of the catalytic convertor of a claus unit. *Gazovaya Promyshlennost*, 9:60–61, 1990.

[12] Detlev Stalling and Hans-Christian Hege. Fast and resolution independent line integral convolution. In *Proceedings of the 22nd annual conference on Computer graphics and interactive techniques*, pages 249–256, 1995.

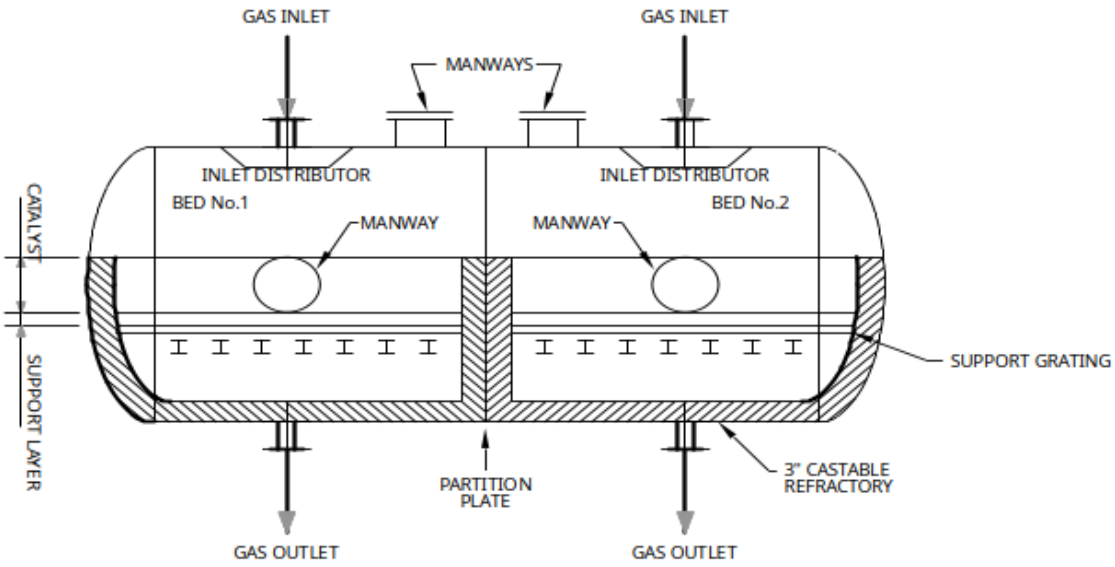

(a) Schematic of a typical two-bed Claus process catalytic converter vessel.

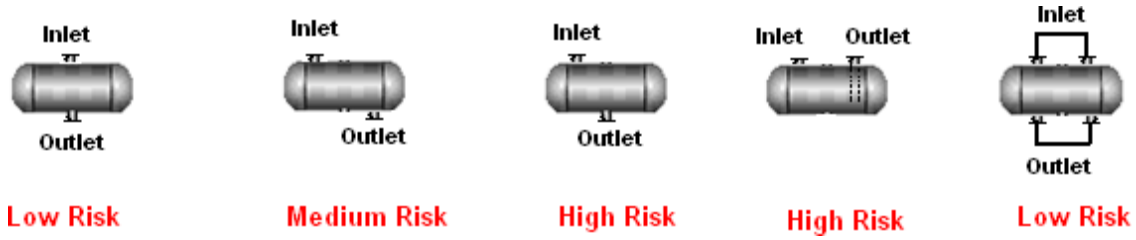

(b) Examples of reactor designs and assigned risk for catalyst displacement.

(c) Example of an inlet impingement plate.

(d) Snapshot of the result of catalyst displacement where catalyst leaked below the support grating.

Figure 2

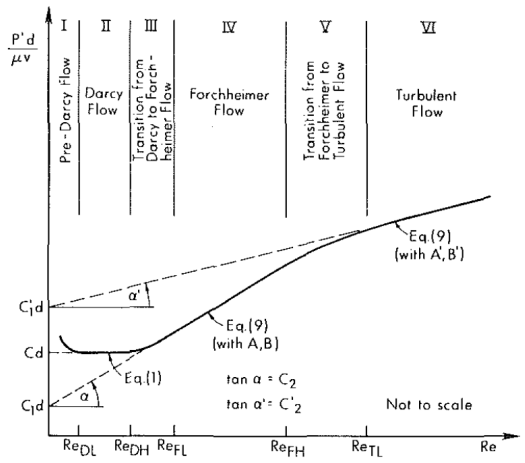

Figure 3: Flow regimes within porous media for fixed particle size and porosity, taken from ref. [9]

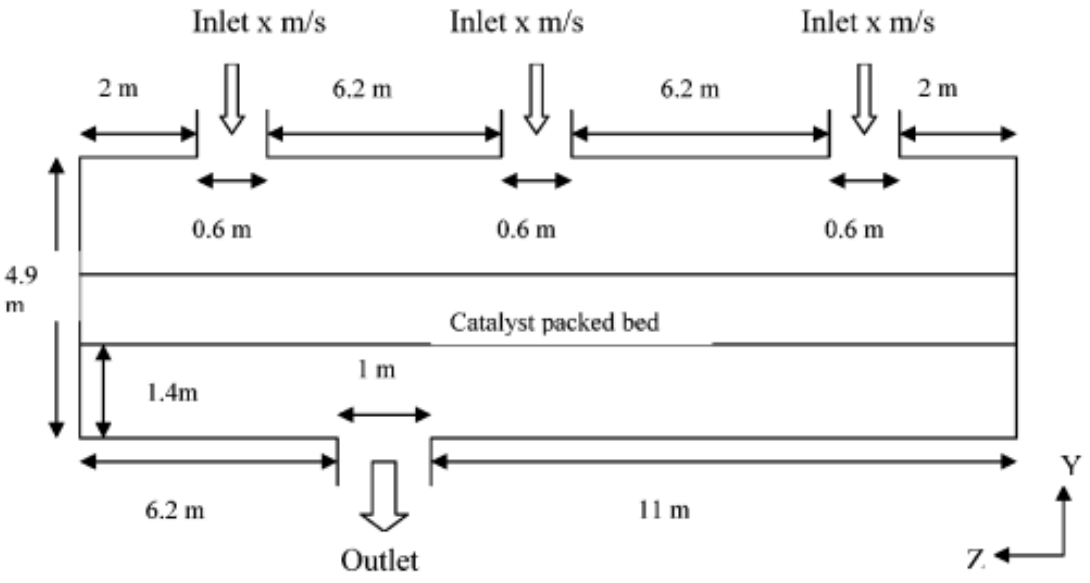

Figure 4: Schematic diagram of a multi-inlet Claus converter take from ref. [2].

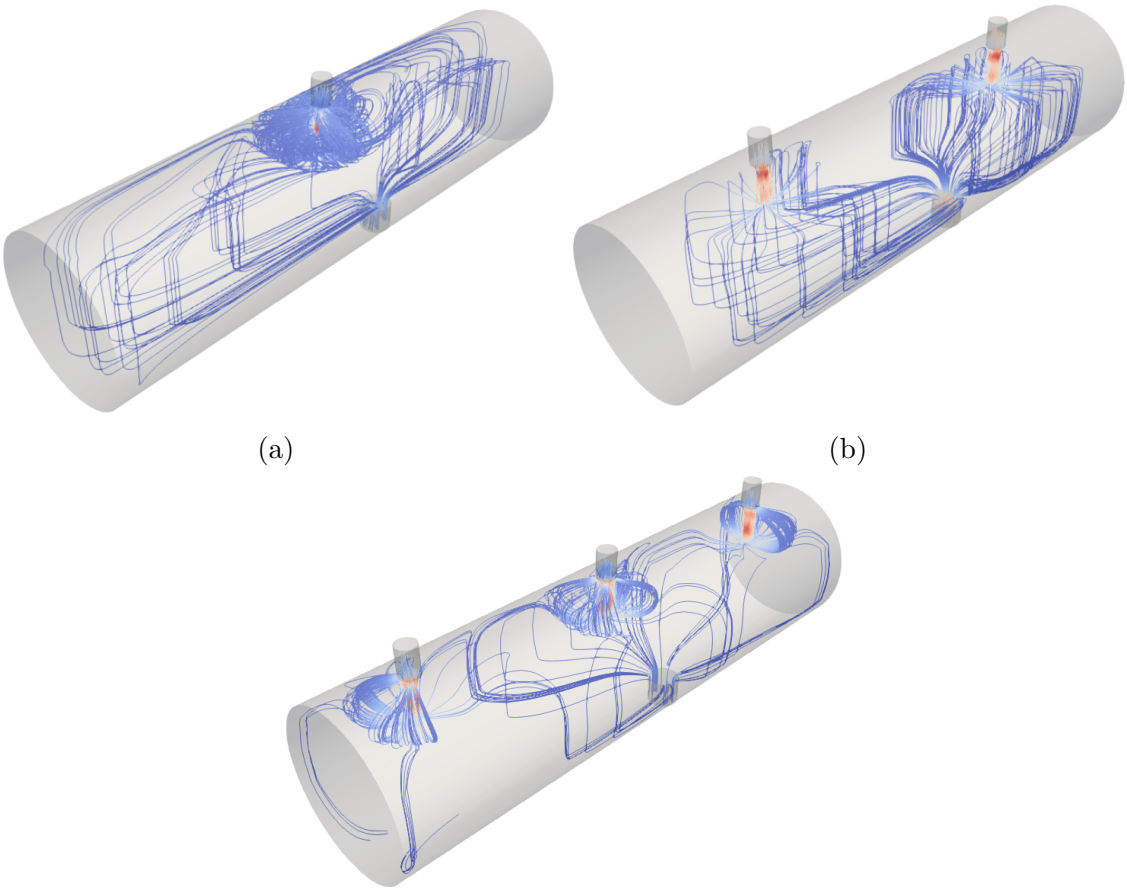

(a) (b)

(c)

Figure 5: Velocity streamlines visualization for (a) single, (b) dual, and (c) triple inlet reactor designs.

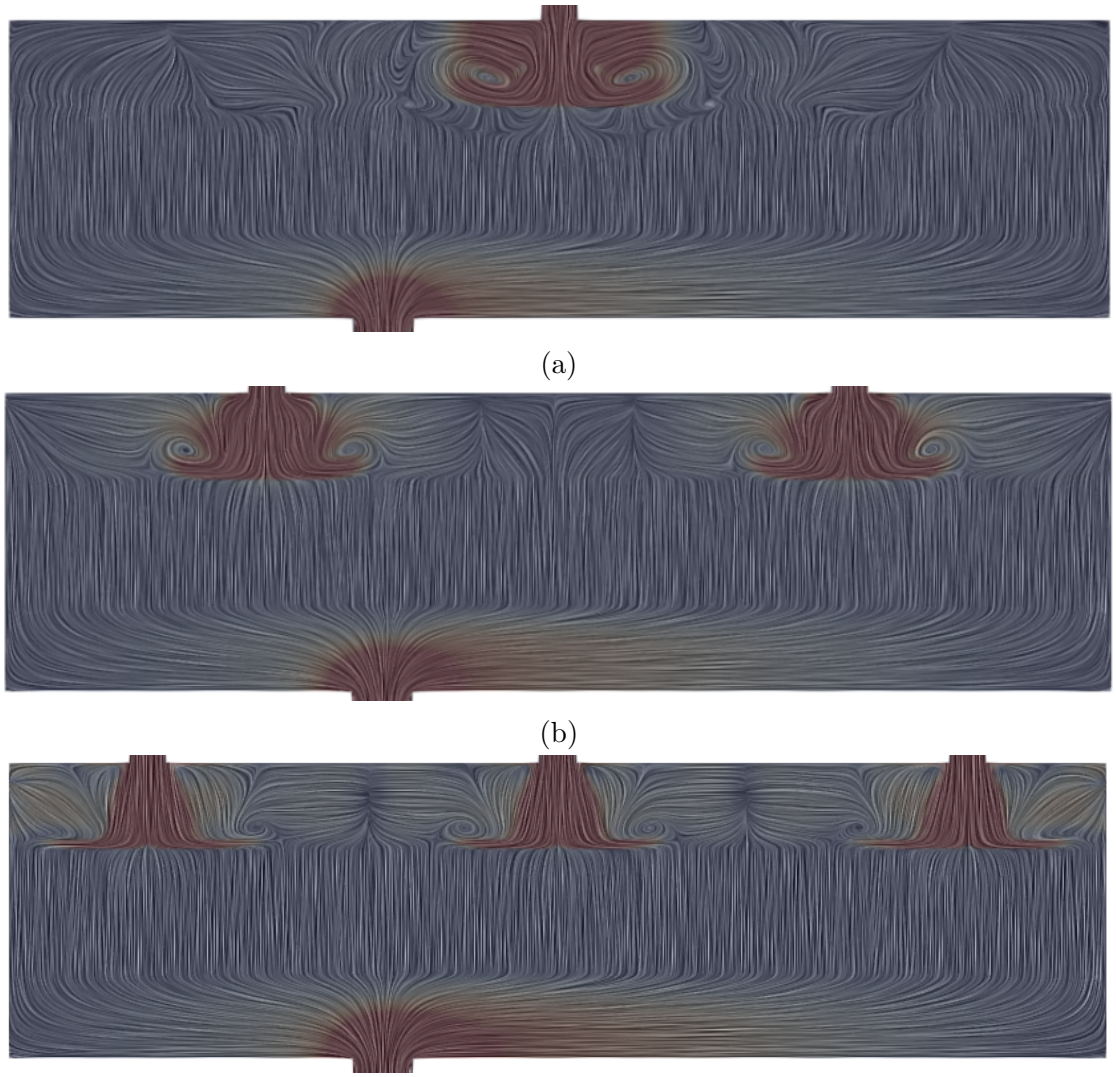

(a)

(b)

(c)

Figure 6: Velocity LIC visualizations for center vertical cross-sections of the (a) single, (b) dual, and (c) triple inlet reactor designs.

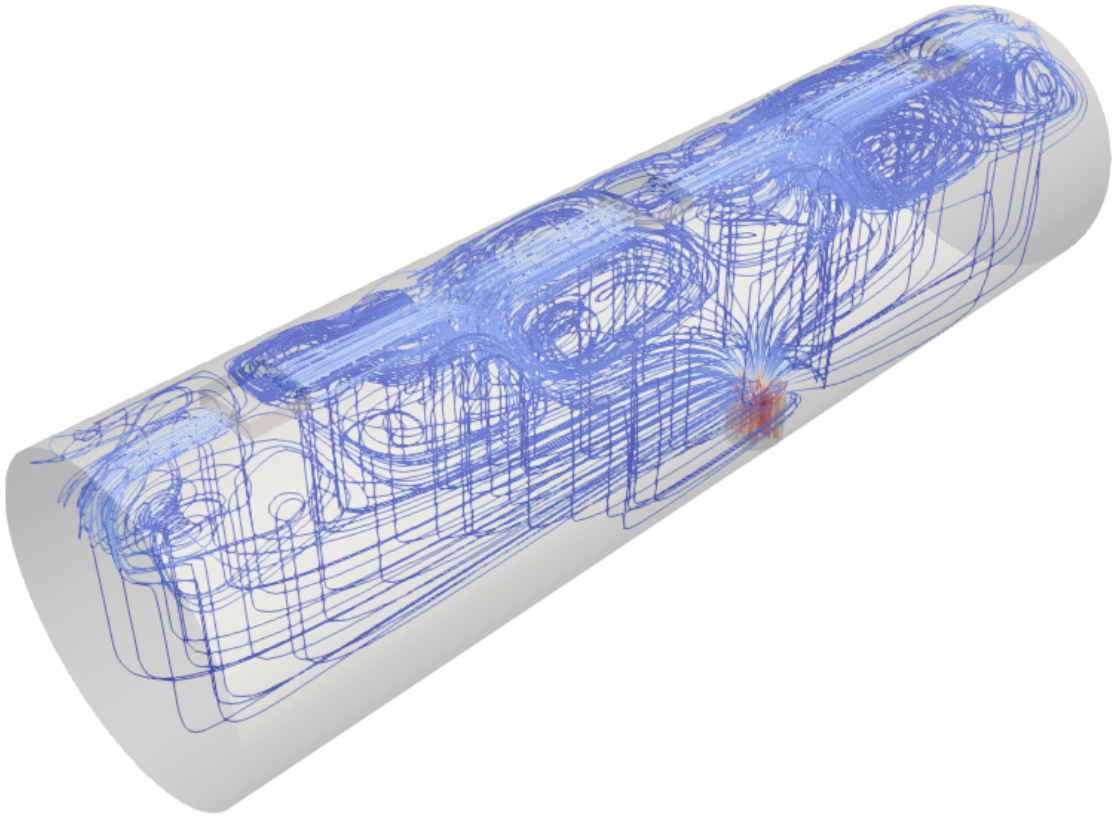

(a)

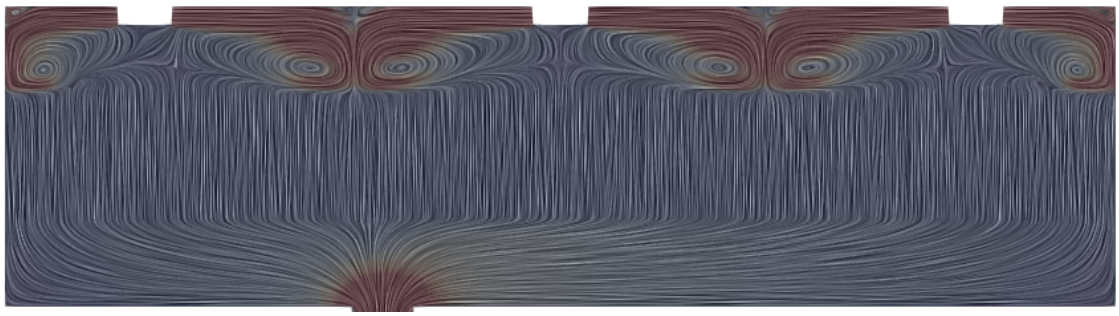

(b)

Figure 7: (a) Velocity streamlines and (b) velocity LIC visualizations for center vertical cross-sections of the triple inlet CRU design with inlet impingement plates.

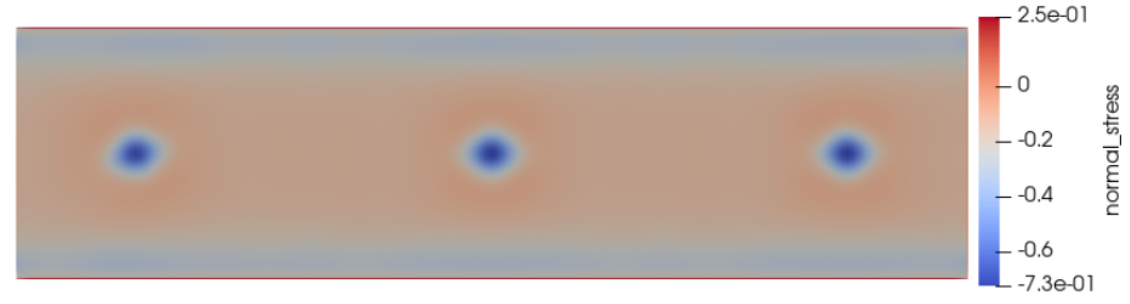

(a)

(b)

Figure 8: Magnitude of normal stresses evaluated at the top catalyst bed/fluid interface for triple inlet designs (a) without and (b) with inlet impingement plates.

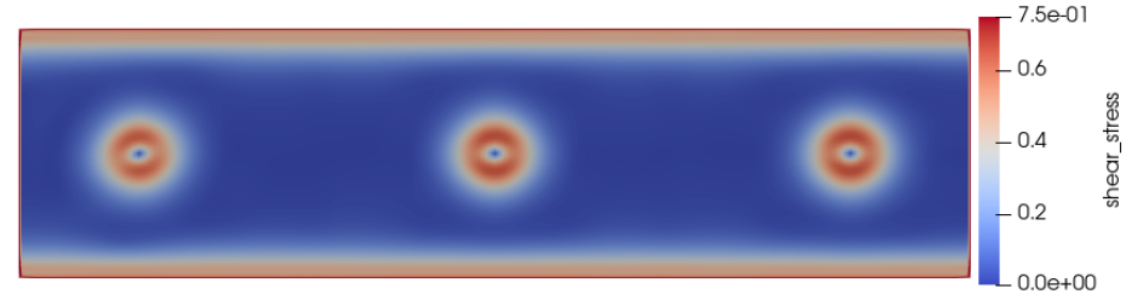

(a)

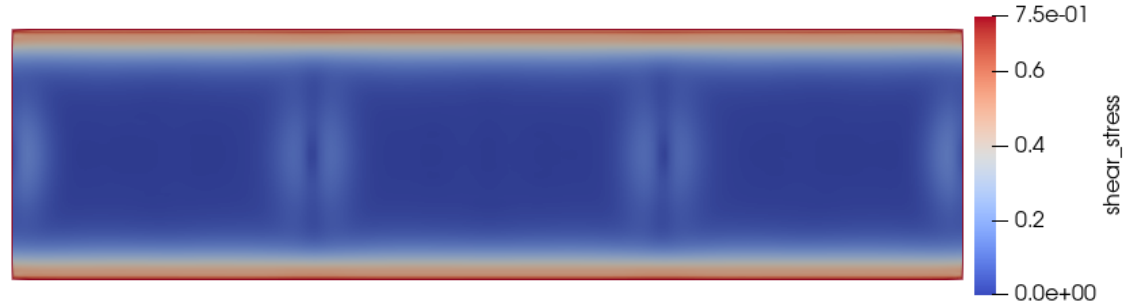

(b)

Figure 9: Magnitude of shear stresses evaluated at the top catalyst bed/fluid interface for triple inlet designs (a) without and (b) with inlet impingement plates.

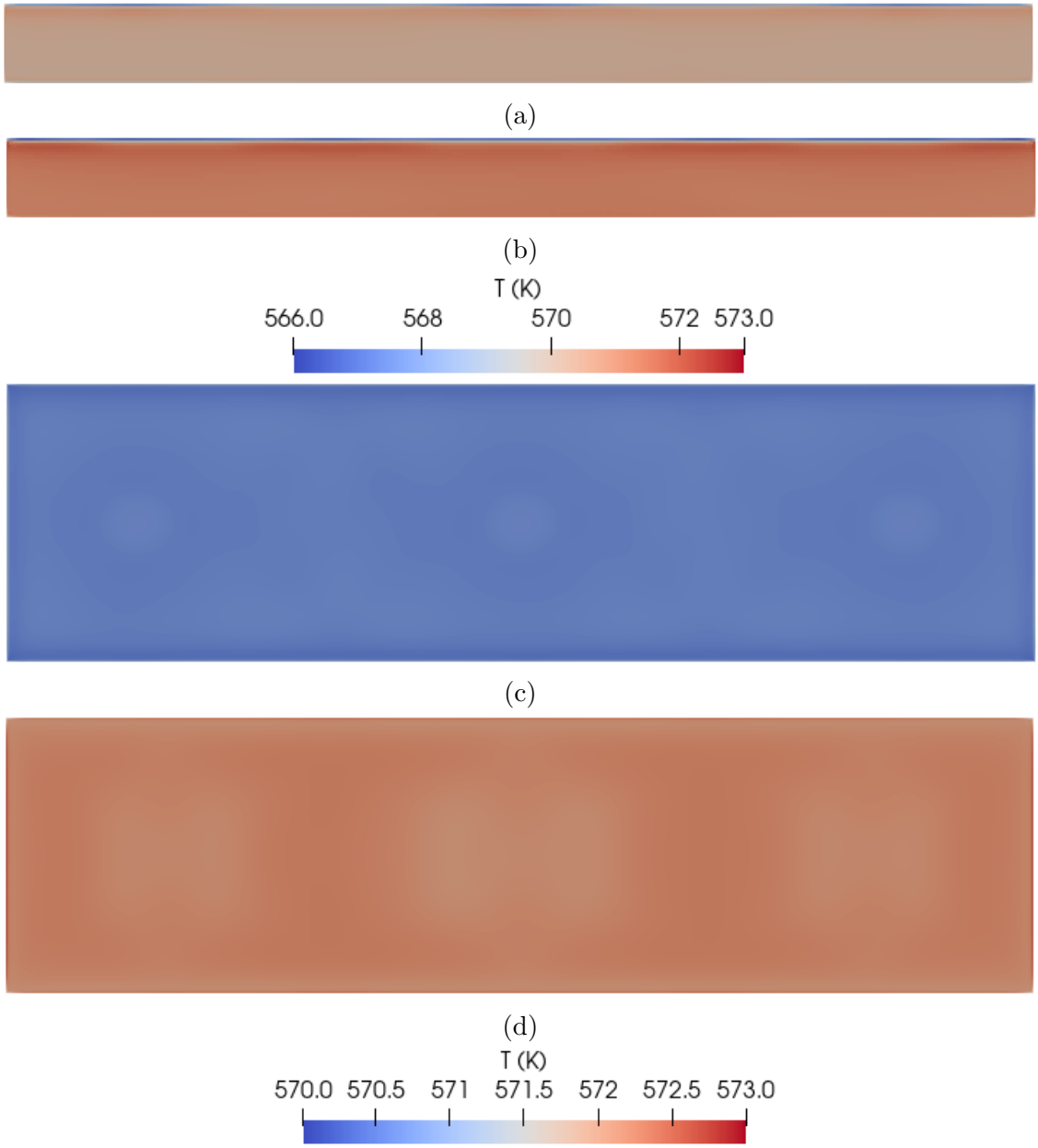

Figure 10: (a-b) Vertical cross-sections of catalyst bed temperature (solid porous phase) for triple inlet designs (a) without and (b) with inlet impingement plates. Horizontal cross-sections of catalyst bed temperature (process gas) for triple inlet designs (c) without and (d) with inlet impingement plates.

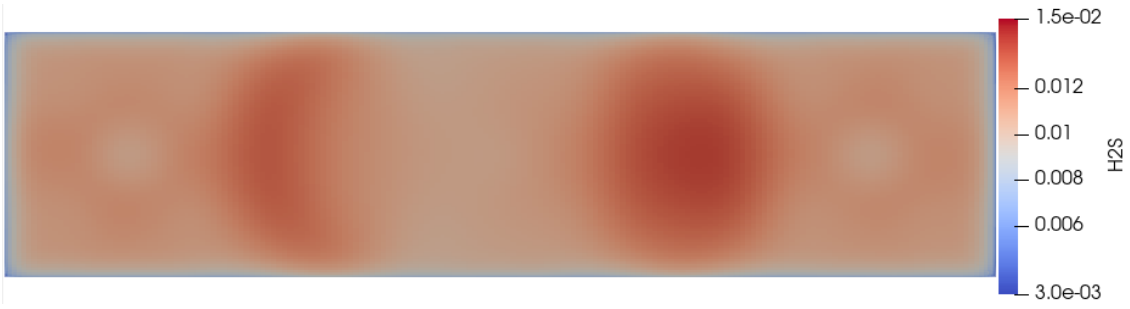

(a)

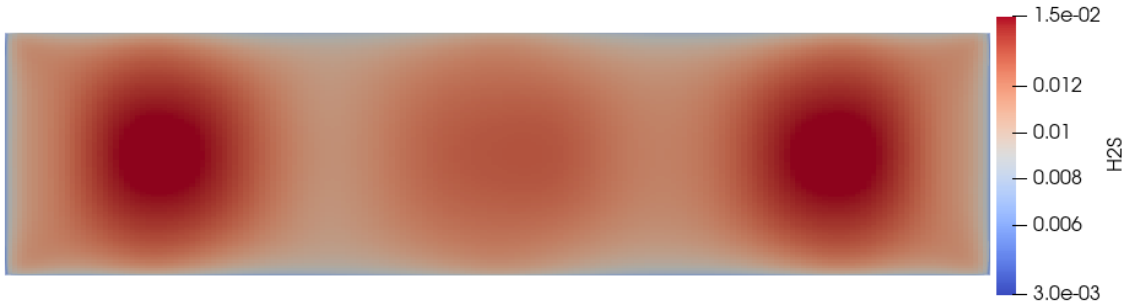

(b)

Figure 11: Horizontal cross-sections of H_2S mass fraction at the outlet of the catalyst bed for triple inlet designs (a) without and (b) with inlet impingement plates.